

Luminescent complexes of the trinuclear silver(I) and copper(I) pyrazolates supported with bis(diphenylphosphino)methane

Supporting Information

A. A. Titov[†], O. A. Filippov[†], A. F. Smol'yakov^{†||‡}, I. A. Godovikov[†], J. R. Shakirova[†], S. P. Tunik[‡], I. S. Podkorytov[§] and E. S. Shubina*[†]*

[†] A. N. Nesmeyanov Institute of Organoelement Compounds, Russian Academy of Sciences, Vavilov Str., 28, 119991 Moscow, Russia

[‡] Institute of Chemistry, St. Petersburg State University Universitetskii pr., 26, 198504, St. Petersburg, Russia

[§] St. Petersburg State University, Laboratory of Biomolecular NMR, St. Petersburg, Universitetskaya nab. 7/9, 199034, Russia

^{||} Inorganic Chemistry Department, Peoples' Friendship University of Russia, Miklukho-Maklaya str. 6, 117198, Moscow, Russia

[‡] Plekhanov Russian University of Economics, Stremyanny per. 36, Moscow, 117997, Russian Federation

Figure S1. ^1H (black) and ^{19}F (red) NMR spectra of complex 2a in CD_2Cl_2 , RT	4
Figure S2. ^1H (blue), $^1\text{H}\{^{31}\text{P}\}$ (red) and $^1\text{H}\{^{109}\text{Ag}\}$ (green) NMR spectra of complex 2a in CD_2Cl_2 , RT	4
Figure S3. $^{31}\text{P}\{^1\text{H}\}$ NMR spectra of complex 2a in CD_2Cl_2 at 273 K.....	5
Figure S4. ^1H (black) and ^{19}F (red) NMR spectra of complex 2a in CDCl_3 , RT.....	5
Figure S5. $^{31}\text{P}\{^1\text{H}\}$ NMR spectra of complex 2a in CDCl_3 at 273 K,.....	6
Figure S6. ^1H NMR spectrum of complex 2a in toluene-d ₈ , RT	6
Figure S7. $^{31}\text{P}\{^1\text{H}\}$ NMR spectra of complex 2a at 273 K(blue), 298 K (green), 333 K (grey), 353 K (red) in toluene-d ₈	7
Figure S8. ^1H (black), ^{19}F (red) and $^{31}\text{P}\{^1\text{H}\}$ (blue) NMR spectra of complex 2b in CD_2Cl_2 , RT.....	7
Figure S9. $^{31}\text{P}\{^1\text{H}\}$ NMR spectra of complex 2b at 292 K (black), 273 K(green), 253 K (grey), 233 K (red), 213 K (blue) in CD_2Cl_2	8
Figure S10. First and second channels of electron density transfer upon formation of complexes 2a and 2b as isosurfaces at 0.002 a.u. (red – depletion, blue – concentration of electron density). H and F atoms are omitted.	9
Figure S11. Channels of electron density transfer #3-#8 upon formation of complex 2a as isosurfaces at 0.001 a.u. (red – depletion, blue – concentration of electron density). H and F atoms are omitted.	10
Figure S12. Channels of electron density transfer #3-#8 upon formation of complex 2b as isosurfaces at 0.001 a.u. (red – depletion, blue – concentration of electron density). H and F atoms are omitted.	11
Figure S13. Eyring plot of "merry-go-round" rate temperature dependence (the data of Table S2 excluding T = 198 K). The best fit corresponds to $\Delta\text{H}^\# = 12 \pm 1 \text{ kcal/mol}$	12
Figure S14. Calculated absorption spectrum of 2a'	13
Figure S15. Calculated absorption spectrum of 2b	13
Figure S16. Schematic Jablonsky diagram for 2b . Ground state (GS) and exited states S ₁ , T ₁ and T ₅ potentials represented by idealized parabolas, vertical emissions – by dashed lines.....	14
Figure S17. Schematic Jablonsky diagram for 2a' . Ground state (GS) and exited states S ₁ , T ₁ and T ₅ potentials represented by idealized parabolas, vertical emissions – by dashed lines.....	16
Figure S18. Electron density transfer maps in the $\text{T}_5 \rightarrow \text{S}_0$, emissions of 2a' (left) and 2b (right) as isosurface at 0.002 a.u. Upon the electronic transition the electron density increases in the blue areas and decreases in the red areas. Hydrogen and fluorine atoms are omitted for clarity.....	16
Table S1. Crystal data, data collection and structure refinement parameters for complexes 2a and 2b.	3
Table S2. Rates of the "merry-go-round" intramolecular dppm exchange process.....	12
Table S3. The TD-DFT data of key electronic transitions of complexes 2a' and 2b	14
Table S4. The impacts of atomic fragments to the singlet vertical excitations of 2a' and 2b	15
Table S5. The impacts of atomic fragments of complexes 2a' and 2b to the S_0 -Tx vertical excitations. Hole corresponds to the distribution in the ground state, electron – to the Tx excited states.....	15
Table S6. Analysis of fragments impacts to the $\text{T}_5 \rightarrow \text{S}_0$ vertical emissions.	15
Table S7. XYZ coordinates of all DFT and TD-DFT optimized species.	17

Table S1. Crystal data, data collection and structure refinement parameters for complexes 2a and 2b.

Compound	2a	2b
Molecular formula	C40H25Ag3F18N6P2	C40H25Cu3F18N6P2
Formula weight	1317.21	1184.22
Dimension, mm	0.20×0.18×0.10	0.33×0.28×0.14
Temperature, K	120(2)	120(2)
Crystal system	triclinic	Triclinic
Space group	P $\bar{1}$	P $\bar{1}$
a, Å	11.6217(8)	10.680(7)
b, Å	11.8522(9)	11.922(8)
c, Å	18.6060(13)	19.238(13)
α , deg.	97.5190(10)	74.079(11)
β , deg.	106.5700(10)	75.740(12)
γ , deg.	107.5490(10)	71.620(11)
V, Å ³	2275.2(3)	2201(3)
Z	2	2
ρ_{calc} , g cm ⁻³	1.923	1.787
Linear absorption (μ), cm ⁻¹	14.61	16.25
Tmin/Tmax	0.660/0.746	0.574/0.746
2 θ max, deg.	60	60
No. unique refl.	42101	39651
No. observed refl. ($I > 2\sigma(I)$)	11870	12260
No. parameters	650	622
R1 (on F for observed refl.) ^a	0.0308	0.0239
wR2 (on F ₂ for all refl.) ^b	0.0746	0.0644
GOOF	1.027	1.029

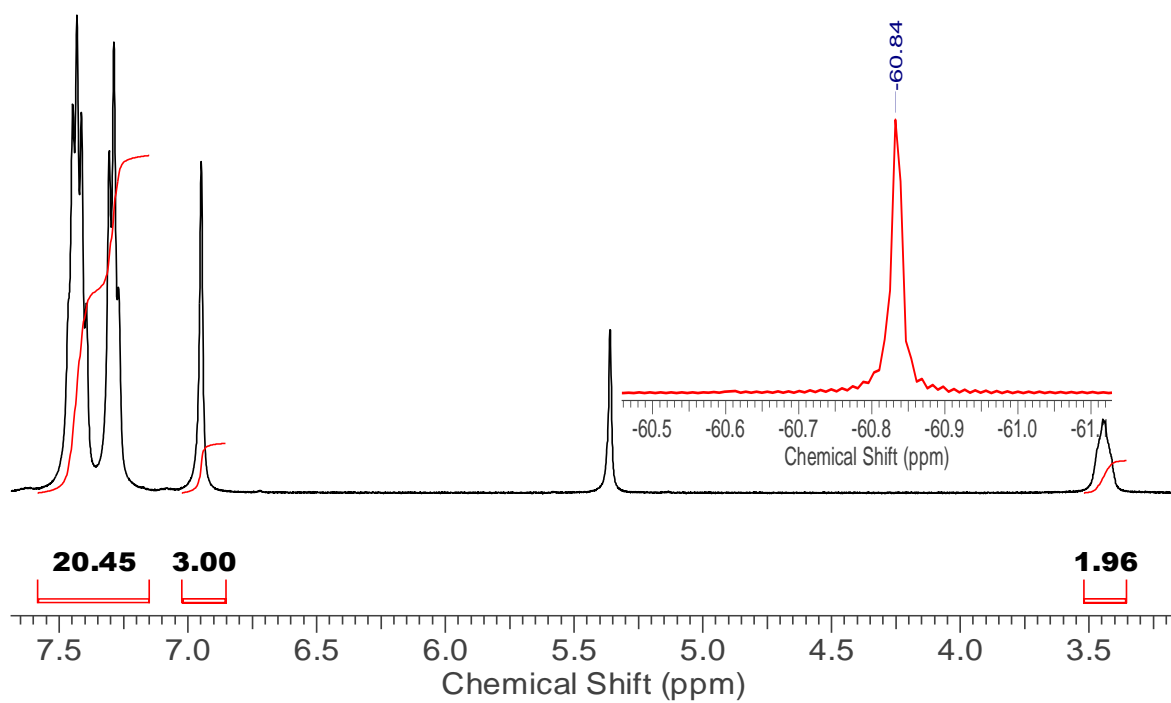


Figure S1. ^1H (black) and ^{19}F (red) NMR spectra of complex 2a in CD_2Cl_2 , RT.

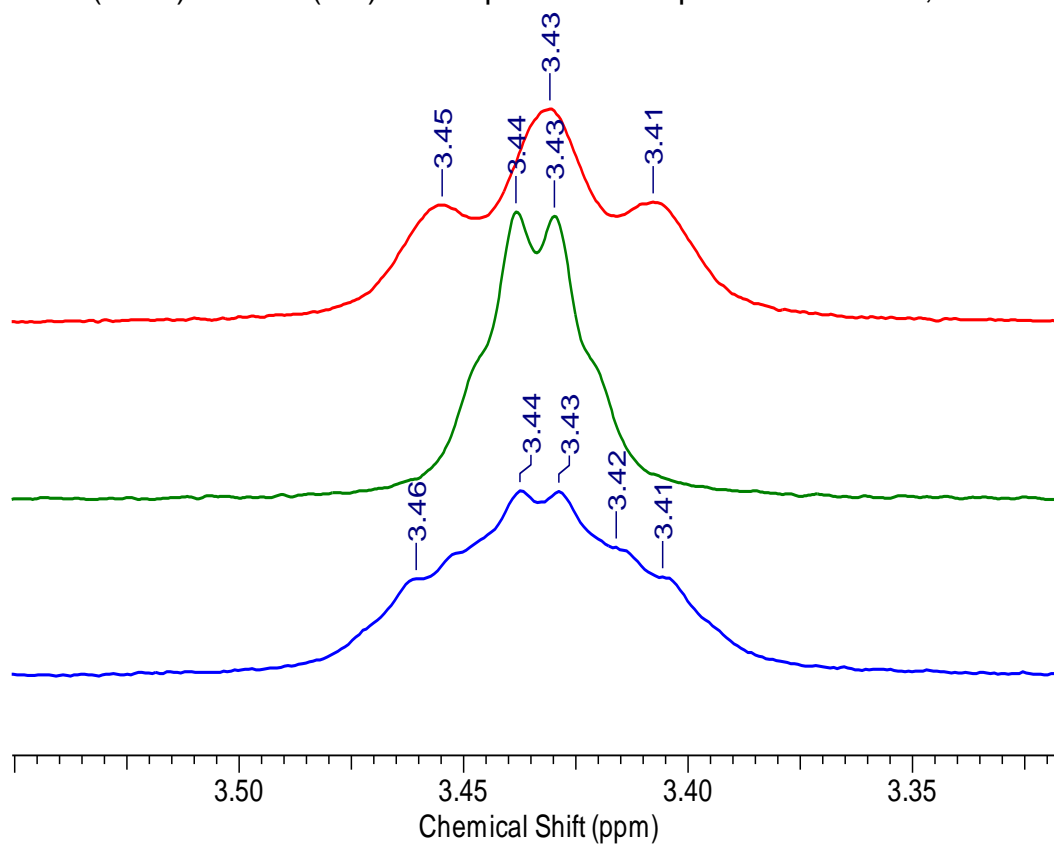


Figure S2. ^1H (blue), $^1\text{H}\{^{31}\text{P}\}$ (red) and $^1\text{H}\{^{109}\text{Ag}\}$ (green) NMR spectra of complex 2a in CD_2Cl_2 , RT

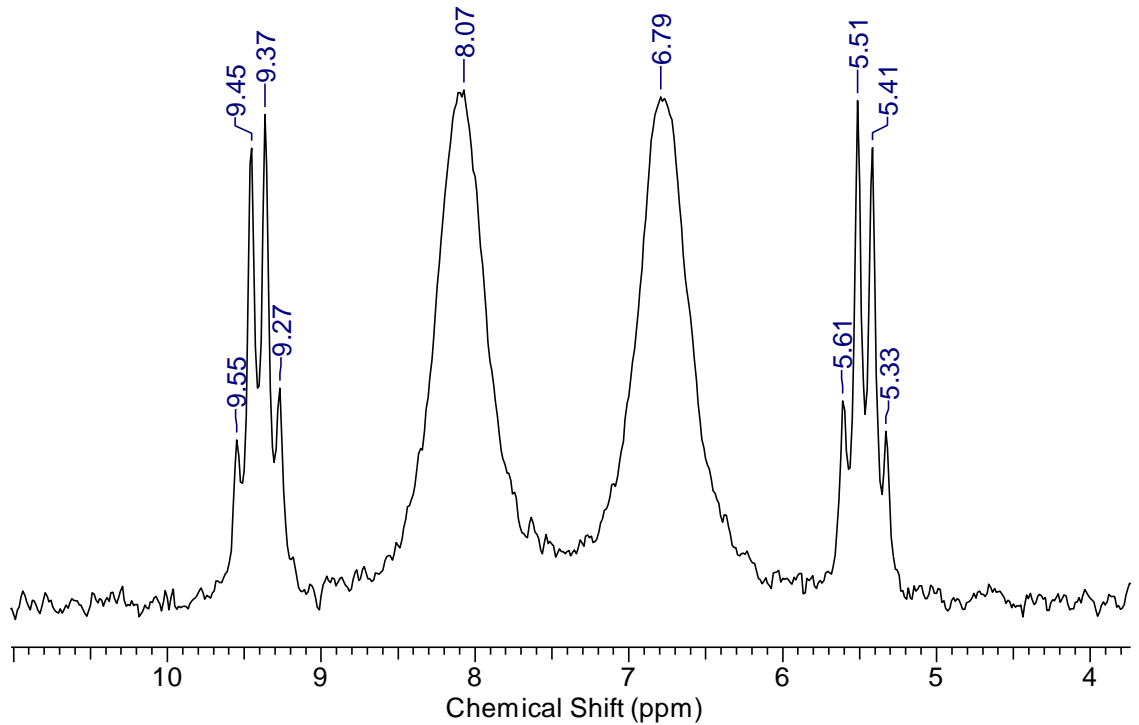


Figure S3. $^{31}\text{P}\{\text{H}\}$ NMR spectra of complex **2a** in CD_2Cl_2 at 273 K.

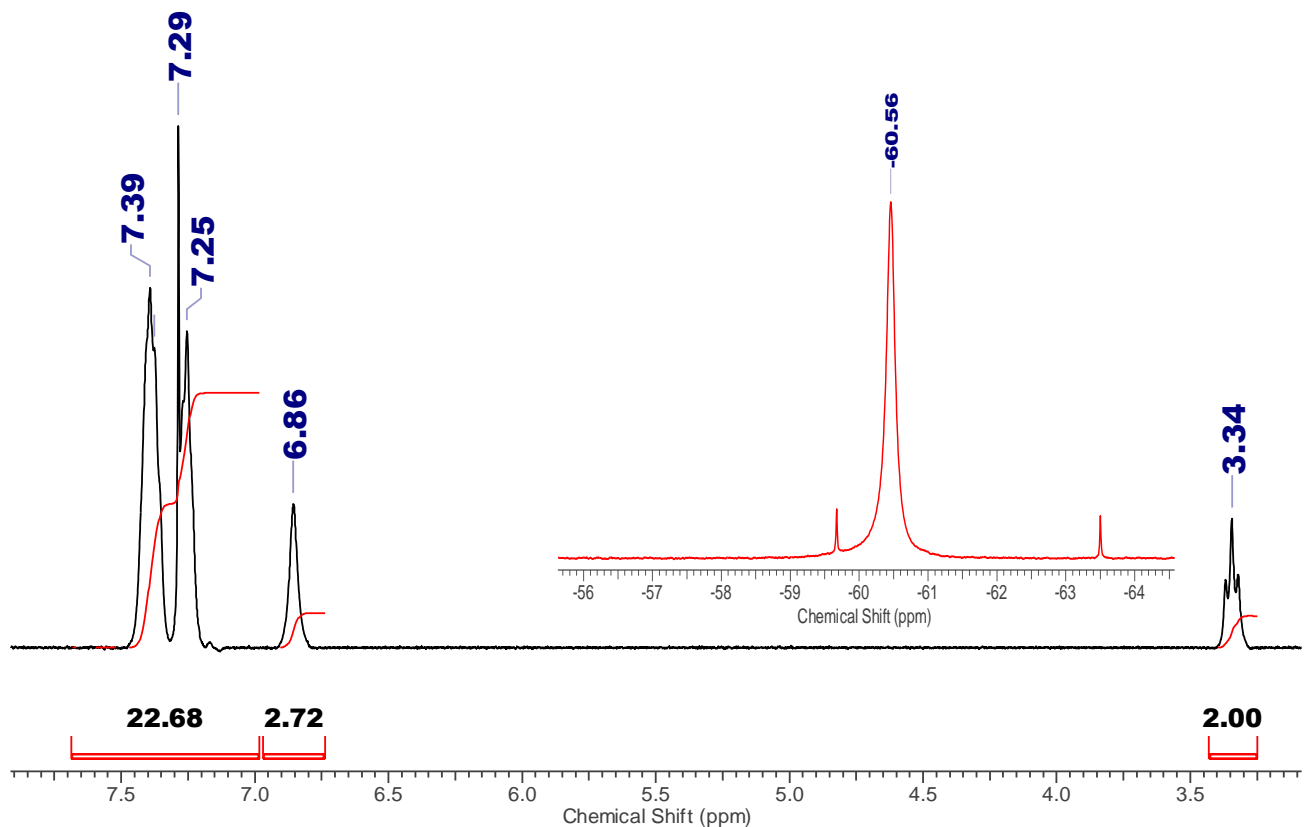


Figure S4. ^1H (black) and ^{19}F (red) NMR spectra of complex **2a** in CDCl_3 , RT.

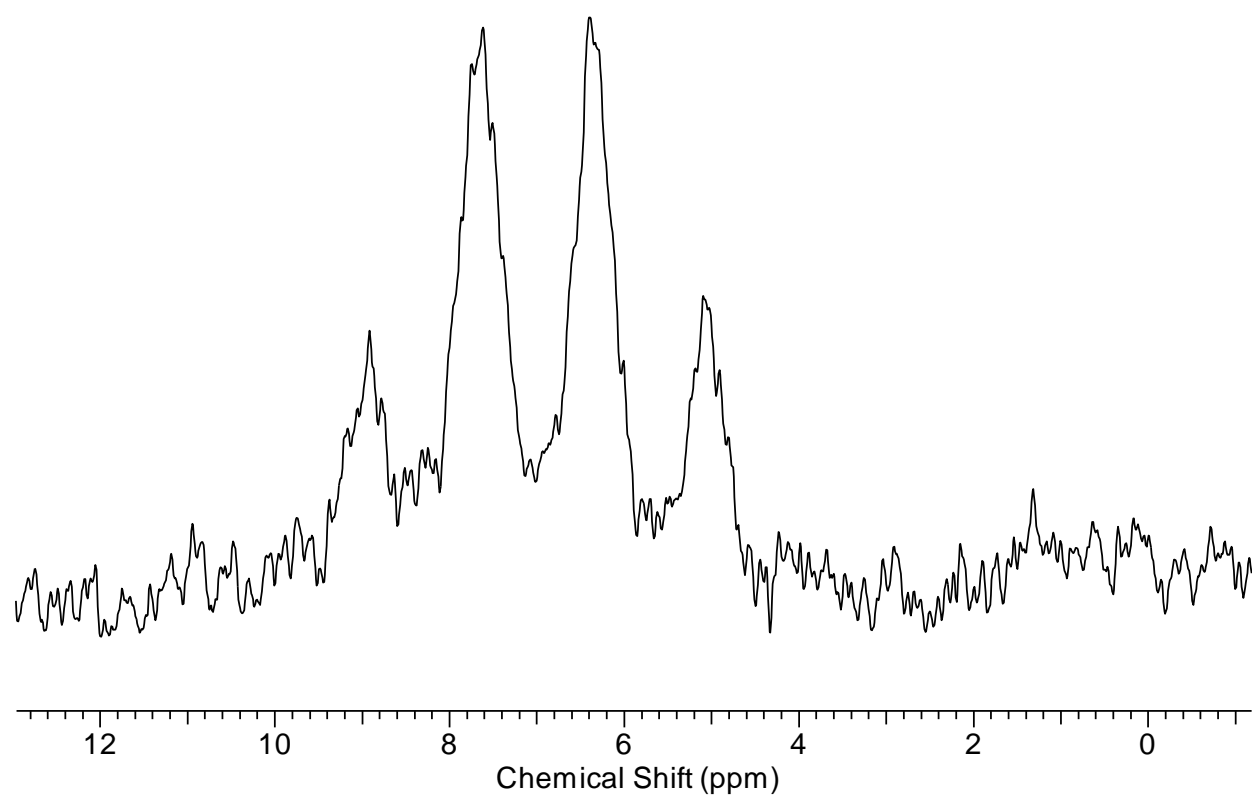


Figure S5. $^{31}\text{P}\{\text{H}\}$ NMR spectra of complex **2a** in CDCl_3 at 273 K,

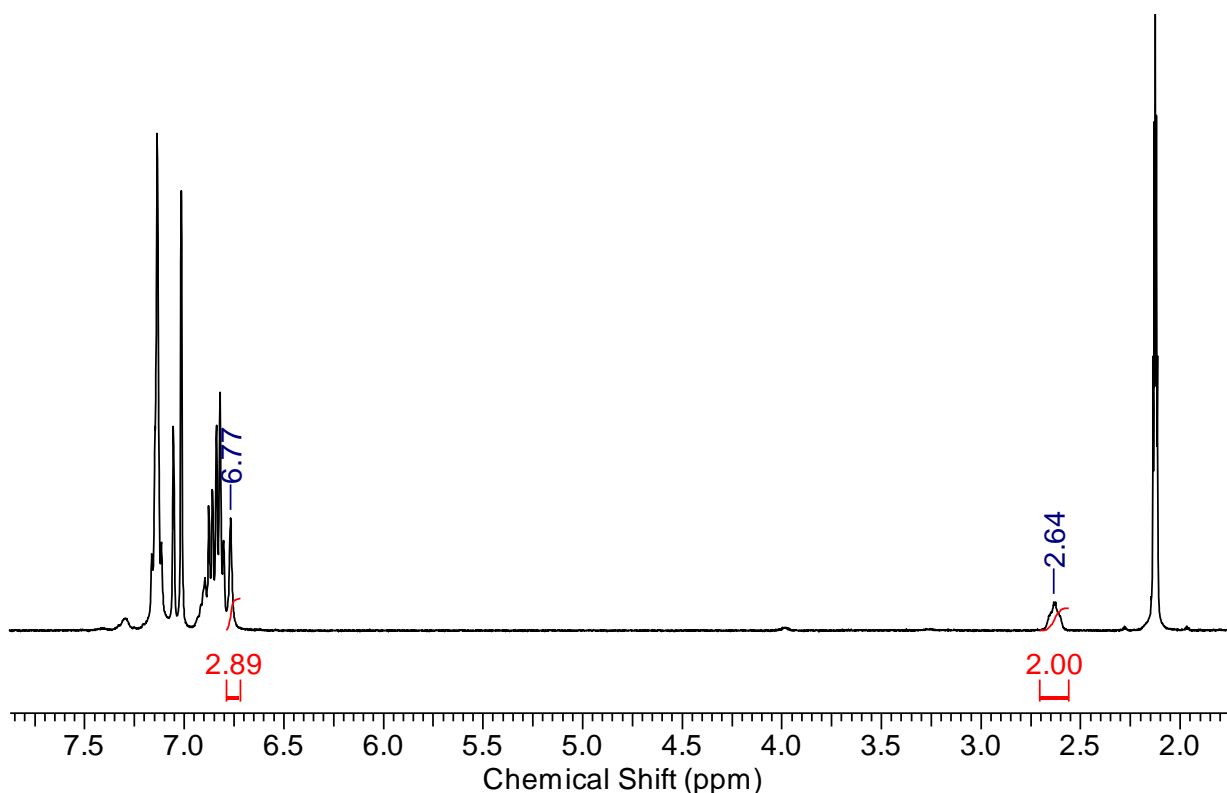


Figure S6. ^1H NMR spectrum of complex **2a** in toluene- d_8 , RT.

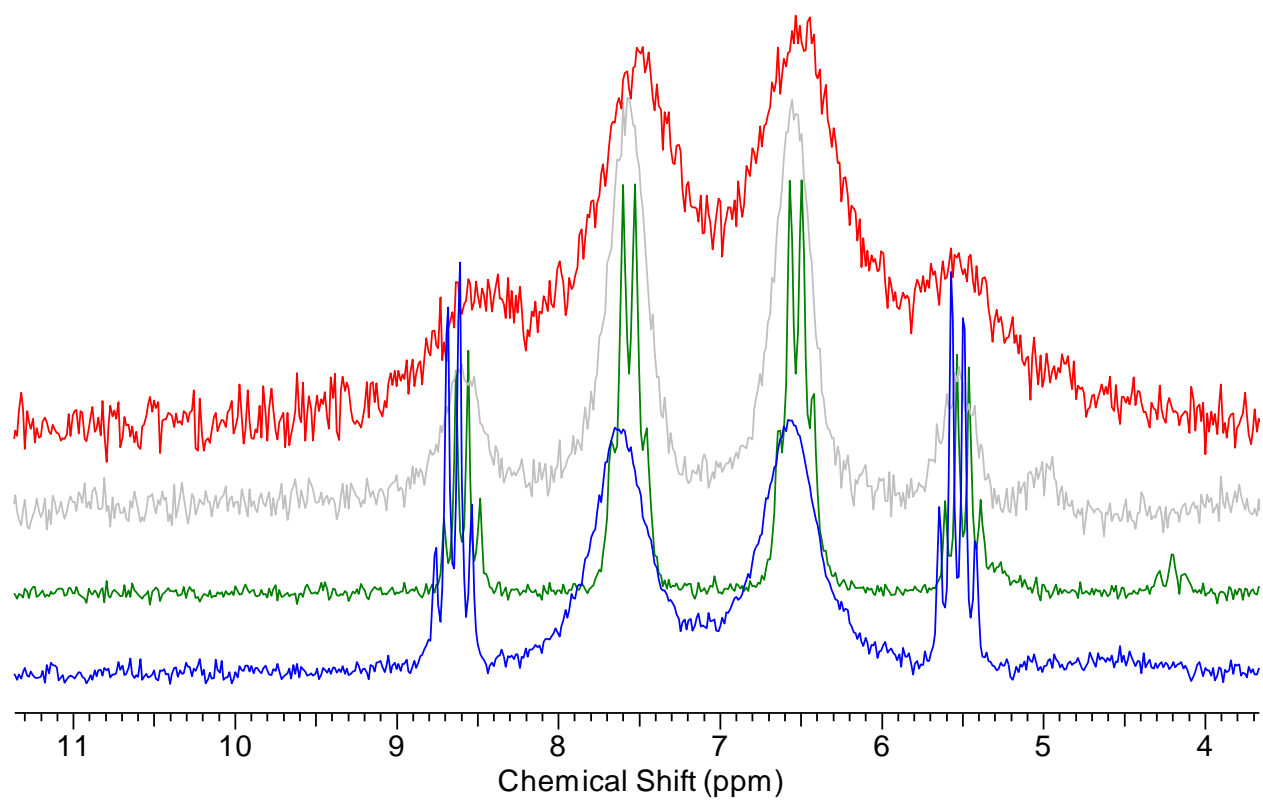


Figure S7. $^{31}\text{P}\{\text{H}\}$ NMR spectra of complex **2a** at 273 K(blue), 298 K (green), 333 K (grey), 353 K (red) in toluene-d₈.

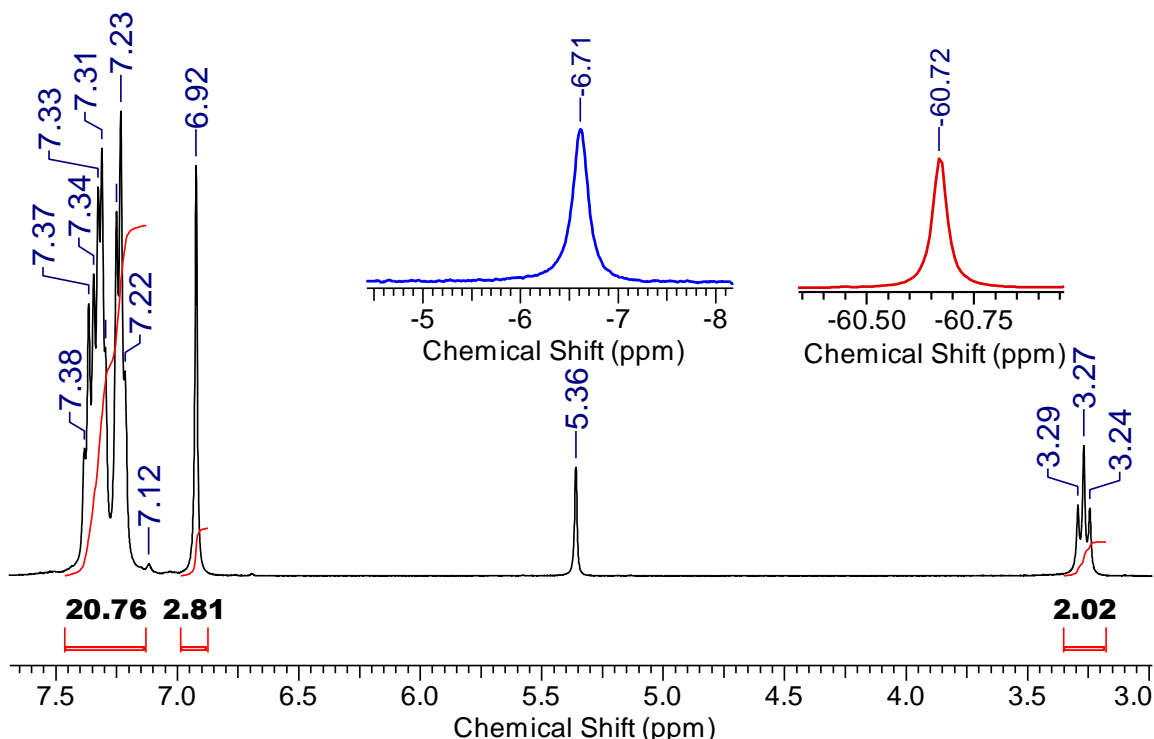


Figure S8. ^1H (black), ^{19}F (red) and $^{31}\text{P}\{\text{H}\}$ (blue) NMR spectra of complex **2b** in CD₂Cl₂, RT.

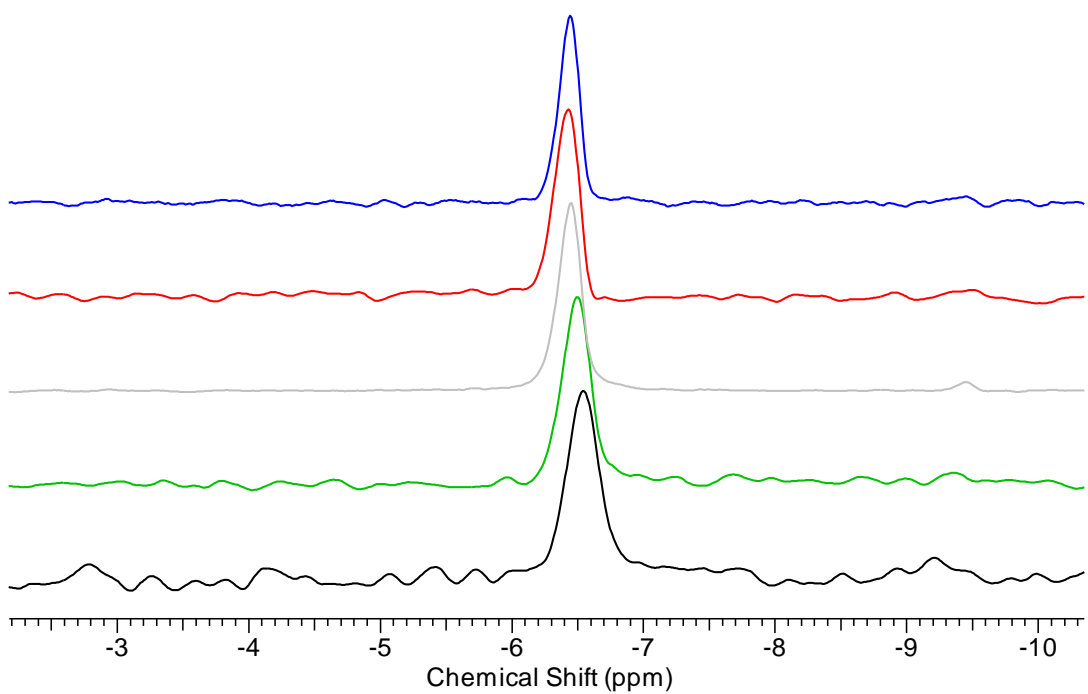
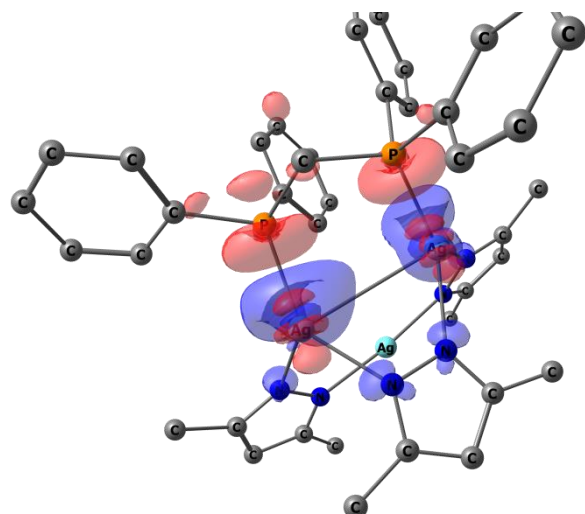
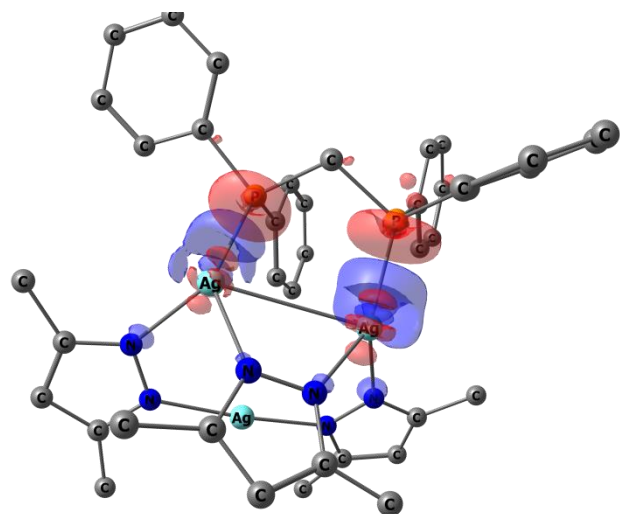


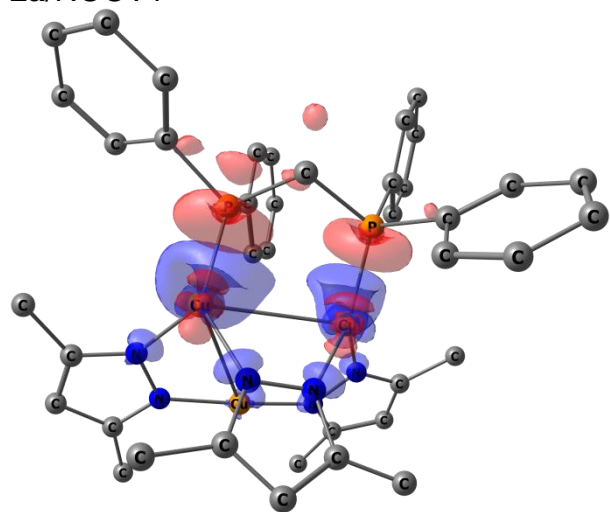
Figure S9. $^{31}\text{P}\{\text{H}\}$ NMR spectra of complex **2b** at 292 K (black), 273 K(green), 253 K (grey), 233 K (red), 213 K (blue) in CD_2Cl_2 .



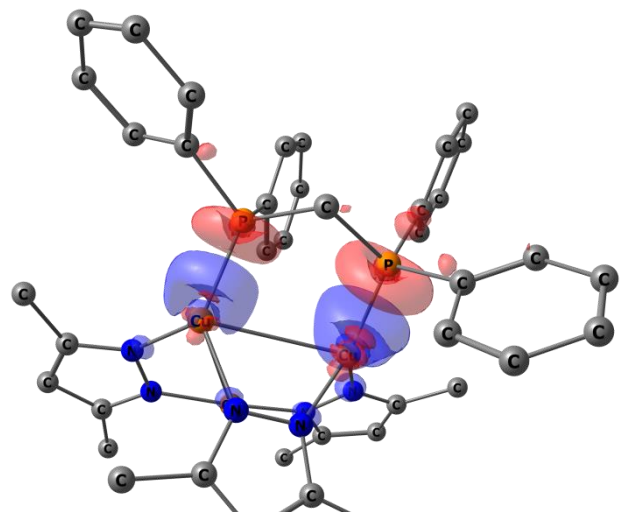
2a/NOCV1



2a/NOCV2



2b/NOCV1



2b/NOCV2

Figure S10. First and second channels of electron density transfer upon formation of complexes **2a** and **2b** as isosurfaces at 0.002 a.u. (red – depletion, blue – concentration of electron density). H and F atoms are omitted.

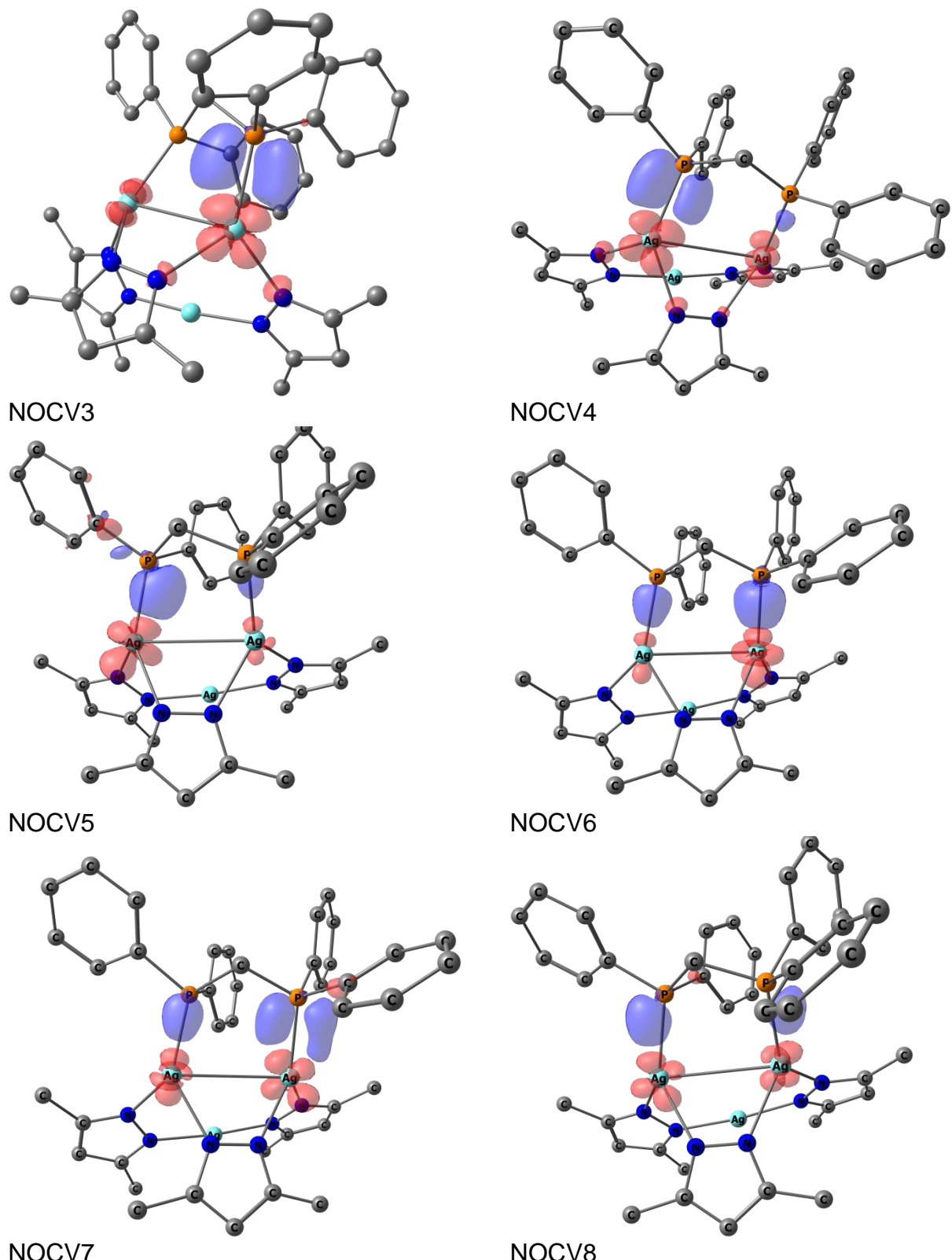


Figure S11. Channels of electron density transfer #3-#8 upon formation of complex **2a** as isosurfaces at 0.001 a.u. (red – depletion, blue – concentration of electron density). H and F atoms are omitted.

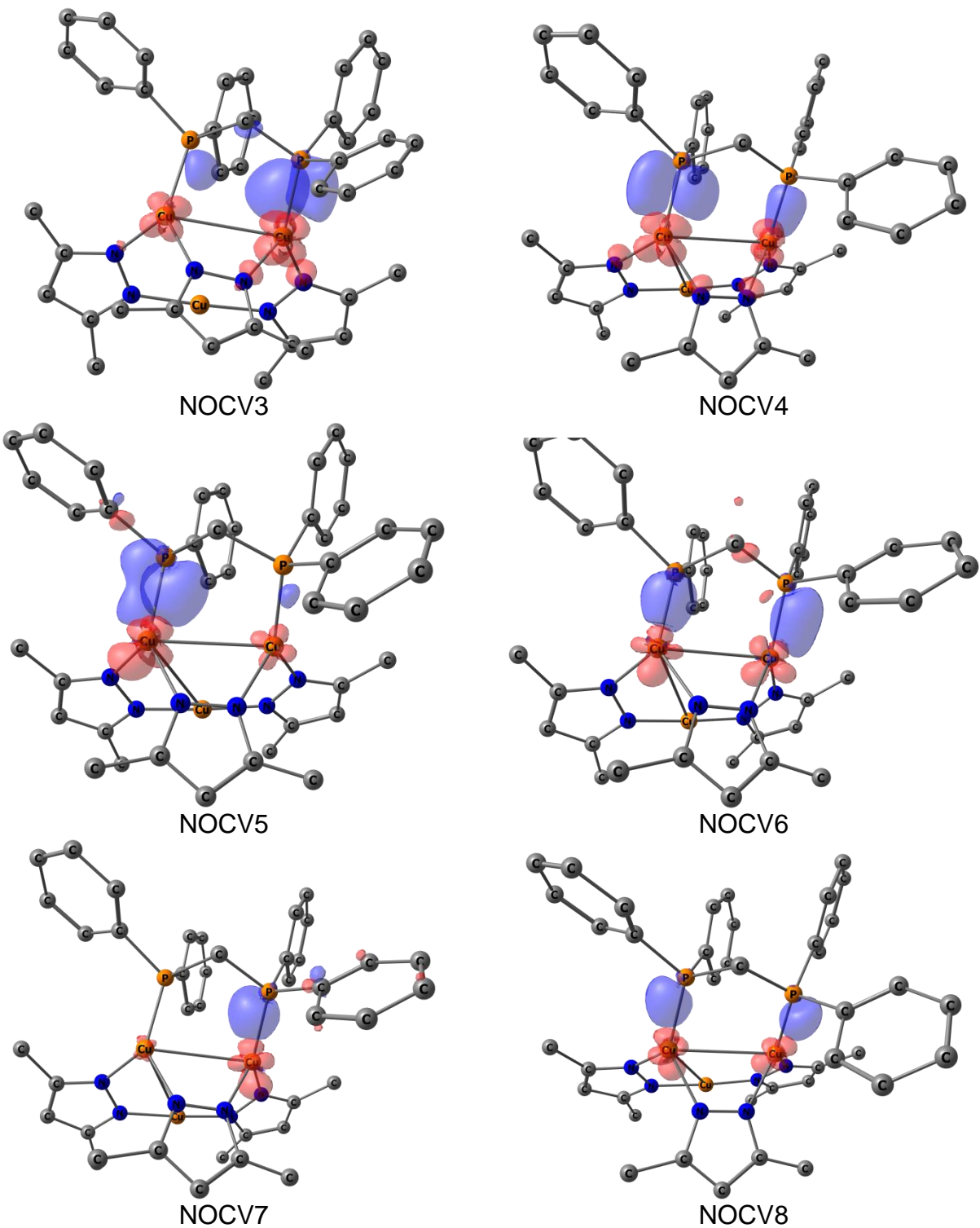


Figure S12. Channels of electron density transfer #3-#8 upon formation of complex **2b** as isosurfaces at 0.001 a.u. (red – depletion, blue – concentration of electron density). H and F atoms are omitted.

Table S2. Rates of the "merry-go-round" intramolecular dppm exchange process

$P(1)Ag(1)Ag(2)P(2) \rightleftharpoons P(1)Ag(1)Ag(3)P(2) \rightleftharpoons P(1)Ag(2)Ag(3)P(2) \rightleftharpoons P(1)Ag(2)Ag(1)P(2) \rightleftharpoons$
 $\rightleftharpoons P(1)Ag(3)Ag(1)P(2) \rightleftharpoons P(1)Ag(3)Ag(2)P(2) \rightleftharpoons P(1)Ag(1)Ag(2)P(2) \rightleftharpoons \dots$
extracted from variable temperature ^{31}P NMR spectra of **2a** by using Spinach program (see Figure 5 and Ref. 20 of the main text).

T / K	k / sec ⁻¹
198	< 0.025 10 ³
218	(0.20 ± 0.05) 10 ³
238	(3.0 ± 0.5) 10 ³
258	(25 ± 5) 10 ³
278	(130 ± 10) 10 ³
298	(450 ± 50) 10 ³

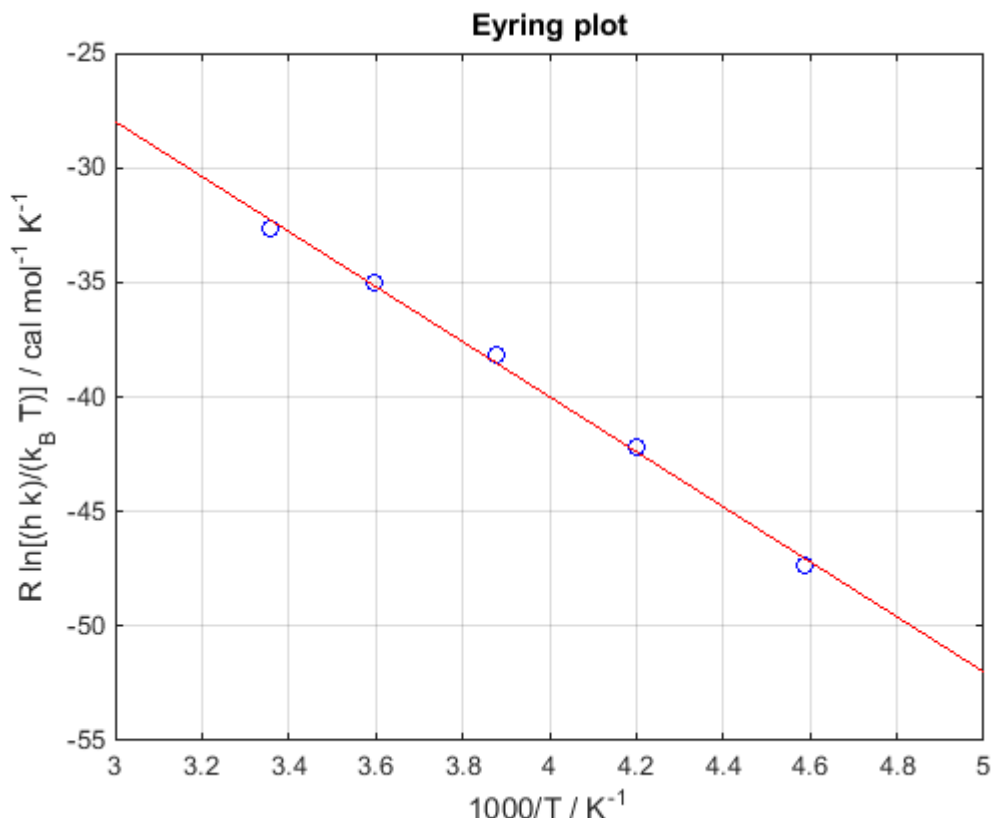


Figure S13. Eyring plot of "merry-go-round" rate temperature dependence (the data of **Table S2** excluding T = 198 K). The best fit corresponds to $\Delta H^\# = 12 \pm 1$ kcal/mol.

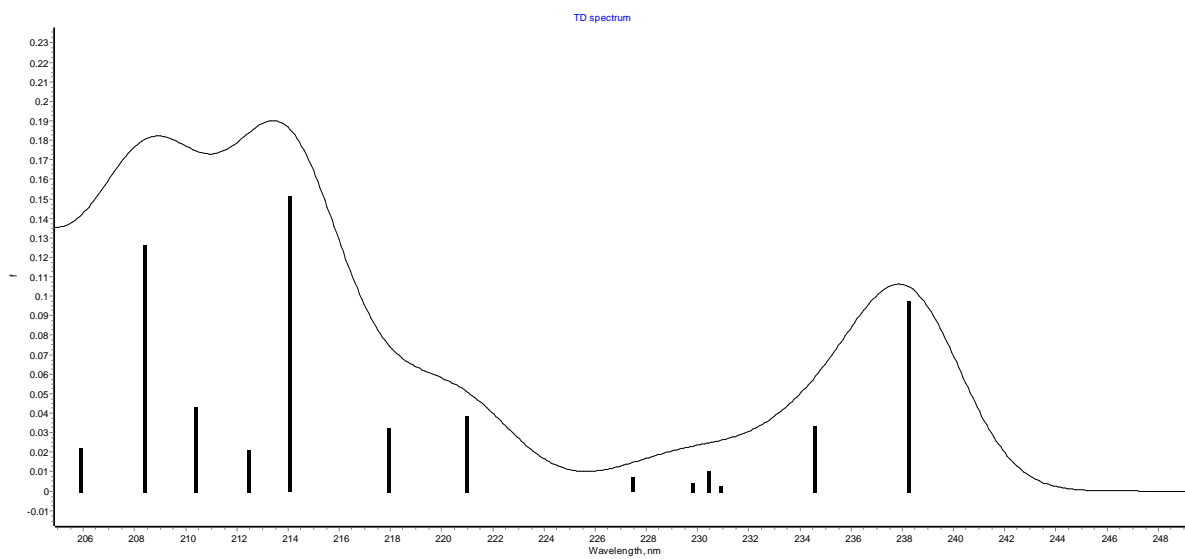


Figure S14. Calculated absorption spectrum of **2a'**.

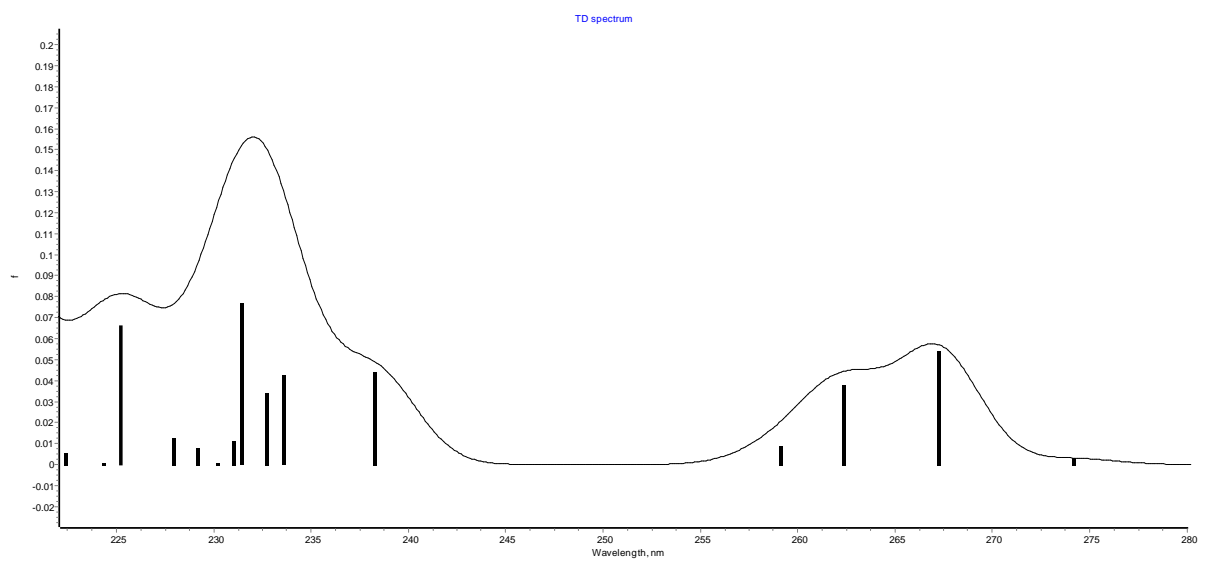


Figure S15. Calculated absorption spectrum of **2b**.

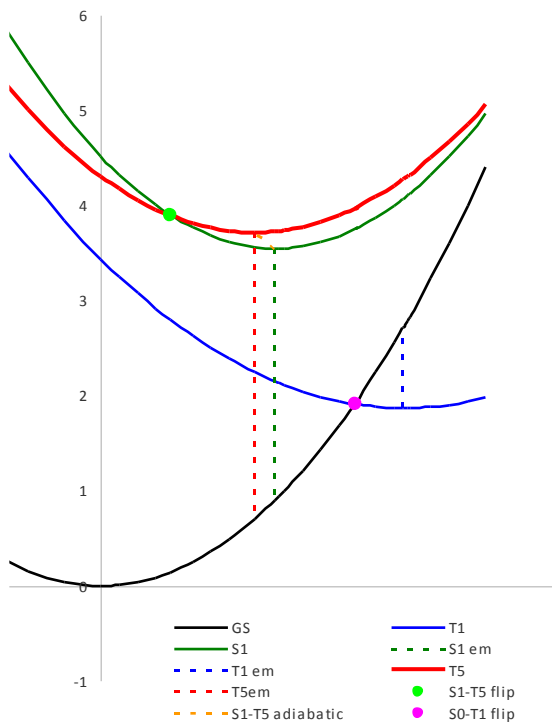


Figure S16. Schematic Jablonsky diagram for **2b**. Ground state (GS) and exited states S_1 , T_1 and T_5 potentials represented by idealized parabolas, vertical emissions – by dashed lines.

Table S3. The TD-DFT data of key electronic transitions of complexes **2a'** and **2b**.

		2b		2a'	
		eV	nm	eV	nm
$S_0 \rightarrow S_1$	Eva	4.52	274	5.20	238
$S_1 \rightarrow S_0$	Eve	2.65	468	3.20	388
	Eadia	3.55	349	4.39	282
$T_1 \rightarrow S_0$	Eve	-0.84	-1471	2.50	496
	Eadia	1.87	663	3.11	399
$T_5 \rightarrow S_0$	Eve	3.02	410	3.11	399
	Eadia	3.72	333	3.84	322

Eva – vertical excitation (absorbance) energy

Eve – vertical emission energy

Eadia – adiabatic energy difference between 2 minima

Table S4. The impacts of atomic fragments to the singlet vertical excitations of 2a' and 2b.

	2b		2a'	
	$S_0 \rightarrow S_2$, E=4.640 eV hole	electron	$S_0 \rightarrow S_1$, E=5.205 eV hole	electron
dppm	28.46	69.65	41.88	91.08
M3	48.87	26.70	30.89	8.27
Pz3	22.66	3.65	27.24	0.64
	$S_0 \rightarrow S_3$, E=4.726 eV hole	electron	$S_0 \rightarrow S_2$, E=5.286 eV hole	electron
	dppm	75.85	59.48	97.29
M3	52.87	20.64	24.09	2.50
Pz3	23.65	3.50	16.42	0.21

Table S5. The impacts of atomic fragments of complexes **2a'** and **2b** to the S_0 -Tx vertical excitations. Hole corresponds to the distribution in the ground state, electron – to the Tx excited states.

		2b				2a'		
	Evex, eV		Hole	Electron	Evex, eV		Hole	Electron
T ₁	3.4395	dppm	72	93	3.4622	dppm	85	98
		M3	23	5		M3	4	2
		Pz3	6	2		Pz3	11	0
T ₂	3.4617	dppm	80	98	3.4705	dppm	87	96
		M3	14	1		M3	3	4
		Pz3	5	1		Pz3	10	0
T ₃	3.4728	dppm	74	97	3.4884	dppm	89	97
		M3	14	2		M3	3	3
		Pz3	12	1		Pz3	7	0
T ₄	3.4819	dppm	83	97	3.4919	dppm	91	95
		M3	10	3		M3	3	4
		Pz3	7	1		Pz3	6	0
T ₅	4.3097	dppm	22	47	4.5202	dppm	6	5
		M3	50	18		M3	9	9
		Pz3	28	35		Pz3	85	86
T ₆	4.3470	dppm	11	13	4.5321	dppm	2	8
		M3	22	9		M3	10	10
		Pz3	68	78		Pz3	87	82
T ₇	4.3832	dppm	20	47	4.5531	dppm	6	11
		M3	49	29		M3	10	6
		Pz3	31	24		Pz3	84	83

Table S6. Analysis of fragments impacts to the $T_5 \rightarrow S_0$ vertical emissions.

	2b		2a'	
	Hole	Electron	Hole	Electron
dppm	5.27	13.05	1.20	3.20
M3	21.26	7.03	12.25	8.78
Pz3	73.47	79.92	86.55	88.02

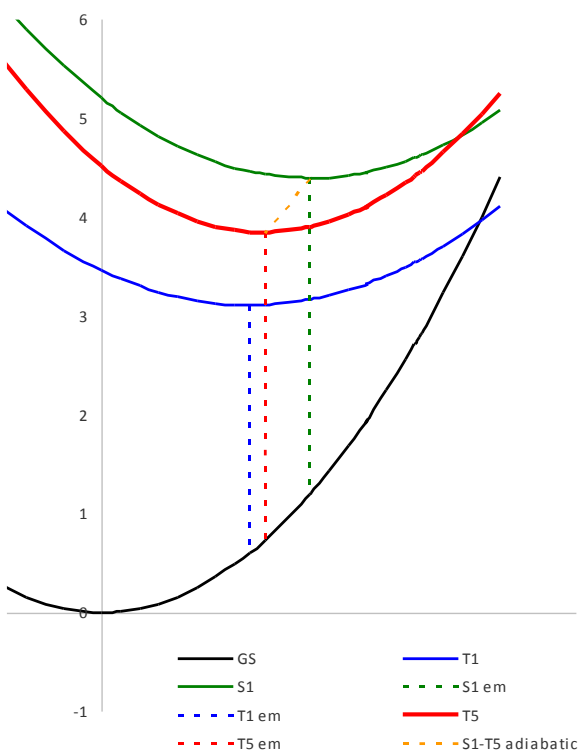


Figure S17. Schematic Jablonsky diagram for **2a'**. Ground state (GS) and exited states S₁, T₁ and T₅ potentials represented by idealized parabolas, vertical emissions – by dashed lines.

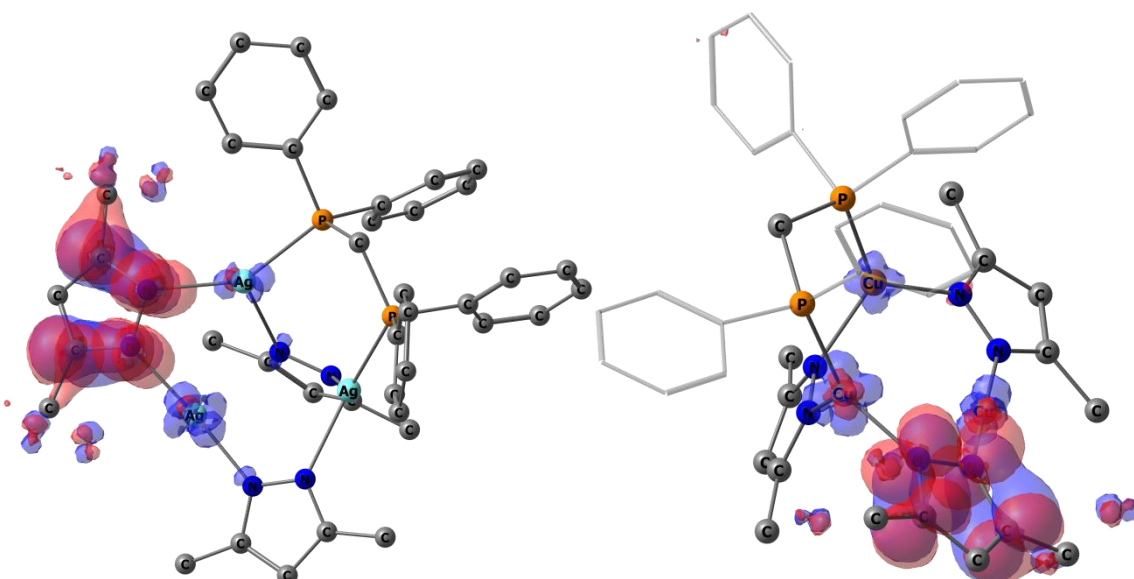


Figure S18. Electron density transfer maps in the T₅→S₀ emissions of **2a'** (left) and **2b** (right) as isosurface at 0.002 a.u. Upon the electronic transition the electron density increases in the blue areas and decreases in the red areas. Hydrogen and fluorine atoms are omitted for clarity.

Table S7. XYZ coordinates of all DFT and TD-DFT optimized species.

2a, PBE/PBE/def2-TZVP, in DCM, EDCM=- 4786.24215783	6	15.432411000	6.907461000	11.315604000
47	10.303684000	11.457387000	14.998590000	6
47	9.915223000	8.797855000	13.120727000	6
47	9.251865000	12.133334000	11.854756000	6
15	12.498166000	10.623106000	15.257283000	6
15	11.838767000	7.822770000	14.097541000	6
9	4.905179000	7.704240000	14.068666000	6
9	10.778316000	14.079551000	16.928818000	6
9	5.802196000	12.069675000	17.284874000	1
9	7.983088000	12.303394000	17.321281000	1
9	6.797212000	13.324601000	15.799012000	1
9	6.921934000	6.887194000	13.807431000	1
9	6.078631000	8.217871000	12.295490000	1
9	8.521910000	6.388514000	11.203357000	1
9	9.399570000	16.970543000	11.243715000	1
9	8.435524000	6.299069000	9.016241000	1
9	7.410815000	11.408936000	7.433707000	1
9	10.238261000	15.125602000	10.413447000	1
9	8.951349000	12.572882000	8.465860000	1
9	8.107017000	15.244715000	10.865275000	1
9	11.142900000	16.199271000	16.504875000	1
9	6.957080000	12.395434000	9.334577000	1
9	10.349412000	6.599265000	10.032223000	1
9	9.124797000	15.506500000	16.963816000	1
7	8.208492000	10.636766000	15.019691000	1
7	9.144536000	9.229497000	11.003621000	1
7	9.627368000	13.822909000	13.022237000	1
7	8.010542000	9.540890000	14.258238000	1
7	8.856963000	10.490253000	10.625706000	1
7	9.887579000	13.693579000	14.337323000	1
6	13.271303000	7.452222000	13.018518000	1
6	13.402556000	11.289336000	16.707359000	1
6	12.567896000	8.791299000	15.500846000	1
6	8.339580000	10.457150000	9.370189000	
6	6.709069000	9.184810000	14.377551000	
6	13.625248000	10.547623000	17.877727000	
6	13.605192000	10.986824000	13.842551000	
6	11.398279000	6.221103000	14.886509000	
6	7.031860000	10.960562000	15.610115000	
6	14.452303000	6.885501000	13.529700000	
6	8.806548000	8.411258000	9.980510000	
6	6.033556000	10.061026000	15.230925000	
6	6.161030000	8.009541000	13.645436000	
6	13.185085000	7.740598000	11.649804000	
6	13.060156000	11.561529000	12.685490000	
6	9.608030000	15.145047000	12.708837000	
6	10.036456000	14.937362000	14.843113000	
6	6.907715000	12.151098000	16.495840000	
6	8.286022000	9.143275000	8.910182000	
6	15.242850000	11.574969000	11.644825000	
6	14.262340000	7.469179000	10.801269000	
6	14.257278000	11.140080000	18.975582000	
6	15.794142000	11.003122000	12.797278000	
6	13.816674000	12.632493000	16.658205000	
6	9.022282000	6.937505000	10.061388000	
6	13.876031000	11.854162000	11.589221000	
6	10.508531000	6.227081000	15.975705000	
6	14.982125000	10.711451000	13.893410000	
2a', PBE/PBE/def2-TZVP, in DCM, EDCM=- 4786.24258283				
47	10.270367000	11.278744000	15.039732000	
47	9.724603000	8.731837000	13.146779000	
47	9.289024000	12.003336000	11.856890000	
15	11.692453000	7.829402000	14.109858000	
15	12.512804000	10.578050000	15.333977000	
9	4.617912000	8.006560000	13.907584000	
9	11.422362000	14.055377000	16.753102000	
9	5.787634000	12.158092000	17.308764000	
9	7.976481000	12.175989000	17.439723000	
9	6.961480000	13.371841000	15.920850000	
9	6.563310000	7.016309000	13.710590000	
9	5.908390000	8.443778000	12.195530000	
9	8.413770000	6.298158000	11.148065000	
9	9.751762000	16.793256000	11.148471000	
9	8.401937000	6.217128000	8.958541000	
9	7.502025000	11.368736000	7.384326000	
9	10.484088000	14.887079000	10.358754000	
9	9.061704000	12.478006000	8.446946000	
9	8.362186000	15.136263000	10.805041000	
9	11.307653000	16.213862000	16.384557000	
9	7.048891000	12.363416000	9.281636000	
9	10.283284000	6.494642000	10.039929000	

6	3.528751000	3.262665000	-2.072320000
6	3.282100000	-2.734830000	-0.540663000
6	-0.631239000	-1.449661000	3.879473000
6	1.823815000	-2.126410000	3.332094000
6	2.617425000	1.097917000	-2.632752000
6	-1.700212000	2.324073000	-2.892425000
6	-3.690970000	-2.403097000	-1.084946000
6	-4.247953000	-0.364969000	-0.574583000
6	-2.916162000	-0.290549000	3.449225000
6	3.009134000	-4.011726000	-0.951992000
6	-0.923700000	3.418739000	-4.896596000
6	3.036148000	1.265877000	-3.951314000
6	-3.023723000	4.901876000	2.270338000
6	0.025457000	4.110857000	-4.148293000
6	-1.863512000	5.340571000	-0.224895000
6	4.577649000	-2.073744000	-0.274836000
6	-1.787665000	2.527631000	-4.266489000
6	3.541033000	3.491364000	1.977012000
6	0.107628000	3.916043000	-2.772856000
6	3.700478000	2.427956000	-4.328832000
6	-4.801539000	-1.571752000	-0.996917000
6	4.883948000	1.807352000	0.894866000
6	-4.909031000	0.947537000	-0.331566000
6	3.951782000	3.425409000	-3.386268000
6	5.861119000	3.221529000	2.588848000
6	-3.161061000	6.139459000	1.647689000
6	-3.623089000	-3.851597000	-1.437337000
6	0.753355000	-5.168599000	-1.557605000
6	-2.583542000	6.355679000	0.398731000
6	4.641260000	3.869688000	2.745280000
6	5.979219000	2.189276000	1.659859000
1	3.711616000	-4.822132000	-1.124354000
1	-5.841084000	-1.807491000	-1.201400000
1	-0.813768000	-1.967592000	4.815699000
1	4.990752000	0.994855000	0.174079000
1	6.931789000	1.670860000	1.533149000
1	6.721271000	3.517625000	3.192864000
1	4.538122000	4.678696000	3.471454000
1	2.597341000	4.017915000	2.122604000
1	-2.228498000	2.908471000	2.134742000
1	-3.486642000	4.718765000	3.242065000
1	-3.729100000	6.936208000	2.132743000
1	-2.698832000	7.321161000	-0.098480000
1	-1.427414000	5.517318000	-1.209685000
1	0.861555000	4.464643000	-2.207389000
1	0.711352000	4.805184000	-4.637654000
1	-0.986924000	3.572304000	-5.976040000
1	-2.532929000	1.980174000	-4.846933000
1	-2.376460000	1.621605000	-2.402328000
1	2.116550000	0.175775000	-2.329029000
1	2.847985000	0.478180000	-4.683539000
1	4.035179000	2.555732000	-5.360616000
1	4.487201000	4.331765000	-3.677401000
1	3.741936000	4.041151000	-1.335266000
1	1.275488000	4.118643000	-0.053195000
1	0.800727000	3.176381000	1.370567000